An Investigation of the Properties of Thick Photoresist Films

Gary E. Flores, Warren W. Flack, Elizabeth Tai

Ultratech Stepper, Inc., San Jose, CA 95134

Process simulation and modeling techniques have demonstrated significant success in predicting the behavior of optical lithography for semiconductor processes with photoresist thicknesses below 2 microns. An extension of these same principles and methods has been applied to thick resist processes up to 10 microns. This study examines the use of simulation analysis in conjunction with experimental results to study the effects of photoresist film thickness and photoresist properties on lithographic performance.

The simulation results examine various photoresist model parameters and their impact on typical lithographic process indicators such as depth of focus and exposure latitude. These results show the importance of the photoresist absorption parameter **A** (μm^{-1}) and the developer selectivity **n** in determining lithographic performance. High values of **n** provide increased process latitude, while low values of **A** reduce the required exposure energy.

The develop rate characteristics and lithographic performance for two commercial photoresist products, Hoechst Celanese AZ 4000 and Shipley STR 1000 were studied over a film thickness range of 2 to 10 microns. Develop rate results show a large difference in the **n** value between these two materials. The cross sectional SEM analysis and Bossung plots indicate that the STR 1000, family has a larger focus and exposure margin than AZ 4000 over the range of film thicknesses. Normalized plots of exposure latitude and depth of focus versus photoresist thickness provide process latitude information. These experimental results support the simulation predictions of the importance of developer selectivity **n** in lithographic performance. Finally, a comparison of different develop rate model parameters was made to study the complex nature of process effects in the development of thick photoresists.

1.0 Introduction

Photoresist films for semiconductor industry applications are typically less than 2 microns in thickness to obtain the necessary resolution and critical dimension (CD) control for etch and implant operations. However, there are an increasing number of applications for thicker photoresist films in the 2 to 20 micron range, which for this study, is defined as “thick photoresist

films." Compared to thin photoresist films, the lithography for thick photoresist films provides a new set of challenges for both process and material optimization.

An example of a thick photoresist application is the fabrication of thin film heads (TFH) for high-performance disk drive systems [1]. As in semiconductor fabrication, CD control for TFH structures is important for performance. However, the large topography present in the typical thin-film head requires the use of photoresist films around 10 microns thick. This results in a loss of CD control due to variations in resist thickness of more than 50% in regions adjacent to large topography [2]. Slopes in the thick resist film also reduce the CD control. There are further detrimental effects on CD control from the specific photoresist optical properties and develop characteristics. First, the bulk absorption effect of the photoresist reduces the effective dose at the bottom of the film. This effect is further impacted by the isotropic wet development process, which produces sloped profiles [2]. Another effect that impacts CD control is highly reflective metal films, which can result in standing wave phenomena. Consequently, the properties of a thick photoresist film will have a dramatic impact on CD control and process latitude.

The semiconductor industry has made extensive use of lithography process modeling to reduce the required experimental work for process optimization and to obtain a better fundamental understanding of complex problems. For example, broadband i-line lithography [3] and deep UV excimer lithography [4] have been successfully modeled using the simulation package PROLITH/2®. While these semiconductor processes involve thin photoresist films, the height-to-linewidth aspect ratios are actually substantially larger for many thick resist applications. This suggests that the lithographic problems associated with thick resist films are just as challenging. Clearly, these applications could benefit from process modeling for the same reasons as semiconductor processes. However, there is scant literature pertaining to lithography process modeling for thick resist films.

An effective technique to study fundamental lithography performance independent of photoresist thickness is to simulate the optical aerial image. A widely used metric for the aerial image is the normalized log slope (NLS):

$$w(\partial \ln I / \partial x) = (w/I)\, \partial I / \partial x \qquad (1)$$

where I is the intensity distribution of the aerial image, w is the feature width and x is the position relative to the image center [5]. This technique can be used to determine the theoretical limit for depth-of-focus (DOF) under various operating conditions. As an example, consider a pattern with a 7 micron pitch that is exposed on a broadband g-h line stepper. Figure 1 shows a normalized log slope versus focal position from nominal (half the DOF) for a series of spacewidths. Using a conservative criterion of a normalized log slope of 6 [5], a spacewidth of 2 microns provides 4.6 microns DOF while a 5 micron spacewidth provides 17.0 microns. Figure 2 shows the effect of numerical aperture (NA) for 4 micron spacewidths. Using the same criteria, an NA of 0.32 would have a DOF of 9.8 microns, while an NA of 0.18 would have a value of 20.4 microns.

It is possible to extend this analysis to approximate the impact of a photoresist film on the theoretical DOF. For example, the above theoretical DOF ranges are based on a specified NLS requirement. A logical extension is then to require a constant NLS throughout the entire photoresist film. This implies that a portion of the DOF range is required to maintain the NLS throughout the film thickness. A first-order approximation to the DOF is to subtract the photoresist film thickness, adjusted for refractive index, from the previous DOF estimates. Figure 3 is a graph illustrating the behavior of DOF versus photoresist thickness for the example of a 4 micron spacewidth with a NA of 0.24. Here the estimated DOF is 14.3 microns. Almost one-third of the theoretical DOF of 20.4 microns is lost in the 10 micron film.

The preceding approach is a useful reference for comparison of the detailed simulations and experimental performance of thick photoresist films. However, the photoresist material properties and develop characteristics will both alter the predictions of DOF. In this study, process simulation will be used to determine the impact of photoresist material properties and develop characteristics on DOF and exposure latitude.

Resist dissolution has been extensively studied to incorporate the photoresist effects in the lithographic process models [6]. However, it is not clear that the existing thin film models will be adequate to describe the behavior of the thick photoresist films. The purpose of this work is to experimentally evaluate two commercial photoresists and to compare the resulting industry standard metrics to the model results. The effect of various modeling parameters will then be presented to illustrate how resist materials could be improved for thick resist applications in the future.

2.0 Process Simulation

2.1 Experimental Design

Process simulation and modeling techniques have demonstrated significant success in predicting the behavior of optical lithography for semiconductor processes with photoresist thicknesses below 2 microns. This approach has been used for initial research into thick photoresist films [7]. Simulation can provide tremendous insight into the crucial photoresist properties that are needed for successful process requirements in thick photoresist applications. The lithography simulator PROLITH/2®, a second generation optical lithography model, was used for all calculation activities in this work, while the imaging system modeled is an Ultratech Stepper Model 1700.

An effective and efficient approach to characterizing multi-factor systems is the use of experimental design methodologies [8]. In a previous study, three photoresist model parameters were varied in a full factorial design scheme [7]. These were the photoresist absorption parameter **A** (μm^{-1}) and two develop model parameters: the developer selectivity **n**, and the maximum development rate $\mathbf{R}_{max}$ (nm/sec) from the Mack develop model [9]. The results indicated that a photoresist absorption parameter **A** equal to 0.40 provided low exposure energies while

maintaining good process latitude. Further, a developer selectivity of **n** equal to 6.0 provided maximum focus and exposure latitude. The maximum develop rate $\mathbf{R}_{max}$ demonstrated insignificant impact on focus and exposure latitude. Both the values of **A** and **n** represent the extreme values in the initial study. Hence, this current work will further explore optimal values of both parameters.

The experimental design utilized in the current study allowed an examination of the effects of **A** and **n** on lithographic performance for a 10 micron thick photoresist film. This approach provided evaluation of a series of theoretical photoresists. A total of six simulation trials, each with unique **A** and **n** values, were studied. Each trial was an extensive focus/exposure matrix characterization of both photoresist critical dimension (spacewidth) and sidewall angle. Table 1 displays the range of conditions used for **A** and **n.** The remaining modeling parameters were assigned the values shown in Table 2. These settings were based on the lithography system, substrate type and standard photoresist properties.

A total focus range of 24 microns centered at -3.3 microns of defocus was simulated for a 4.0 micron spacewidth. The theoretical DOF was estimated in the previous section to be 20.4 microns for a 4.0 micron spacewidth. The -3.3 micron defocus corresponds to the isofocal point for a 10 micron film, or a focus 1/3 of the distance into the film. The remaining focus settings of -15.3, -11.3. -8.3, 0.7, 4.7 and 8.7 microns were then selected symmetrically around the -3.3 micron isofocal setting. Exposure ranges for the focus/exposure matrix were varied from 200 to 3000 mJ in appropriately small increments. These conditions provided a broad view of the process window at each unique photoresist condition.

2.2 Exposure Dose and Latitude

The required exposure dose to achieve a nominal mask spacewidth of 4.0 microns (dose to size) was determined for each simulation at -3.3 micron defocus. Figure 4 displays a contour plot of the behavior of dose to size as a function of **A** and **n** It is evident that increasing **A** results in larger dose to size, while increasing **n** has a relatively small effect. For the extreme conditions of **A** equal to 0.6 and **n** equal to 6.0, dose to size requirements are in the 1800 mJ/cm^2 range, which is four times the value required for **A** equal to 0.2 and **n** equal to 3.0. In particular, there is a flat region of low exposure dose requirements below **A** values of 0.4.

A normalized exposure latitude ($E/\Delta E$) was also determined for each simulation focus/exposure matrix. This is defined as the exposure energy (E) required to achieve a spacewidth of 4.0 microns, divided by the exposure range for ±10% spacewidth control (ΔE). A contour plot in Figure 5 shows the dependence of normalized exposure latitude on **A** and **n**. The general behavior of the contour is an enhancement in normalized exposure latitude from 0.5 to over 1.25 with increasing values of **n**. For conditions of **A** near 0.4 and the large values of **n** near 6.0, there is a maximum normalized exposure latitude of 1.25.

2.3 Focus/Exposure Results

A comparison of the simulated Bossung curves at the four conditions of the experimental design are shown in Figure 6. All the results are displayed in terms of normalized critical dimension, focus and exposure energy. This approach provides an illustrative format for comparing process latitudes among the photoresist design conditions and is useful when comparing the performance of different photoresist thicknesses. The critical dimension (CD) and focus data (F) was scaled by the spacewidth (S) to create a normalized CD (CD/S) and normalized focus (F/S). The exposure energy (E) was scaled by the nominal exposure (E_n) to create a normalized exposure (E/E_n). Hence, for the case of a 4.0 micron spacewidth, a normalized CD increment of 0.1 corresponds to 0.4 microns, and a normalized focus increment of 1.0 corresponds to 4 microns.

For both focus and exposure latitude, conditions of **A** equal to 0.2 and **n** equal to 3.0 illustrate inferior performance to the other three simulations, although there is a low exposure dose to size requirement of 450 mJ. The behavior of the curves further shows a size bias requirement of approximately 10% or 0.4 microns to achieve maximum normalized DOF. At a normalized exposure near 1, which is the nominal CD, there is shallow DOF. The isofocal exposure conditions occurs at a normalized exposure energy of 1.18 and a CD bias of 1.1. There is an improvement in exposure latitude with increasing size bias in the region of a normalized CD of 1.1 to 1.25. However, there is a significant degradation in DOF. Hence, this photoresist design provides insignificant overlap of the maximum DOF and exposure latitude ranges. This suggests these conditions of low optical absorbance and low developer selectivity result in inferior performance for a thick photoresist film. The low optical absorbance probably causes a severely degraded PAC latent image, while the low develop selectivity further exacerbates this effect due to large lateral dissolution of the photoresist profile.

Increasing the value of the develop selectivity **n** to 6.0 shows an improvement in both the DOF and exposure latitude over the previous design. With increasing exposure dose, there is less degradation in the DOF. Also, the maximum normalized DOF occurs at a normalized CD of just below 1.1. Thus there is a reduction in the isofocal energy to 1.07 from the previous conditions of a of 1.18. However, these benefits incur the penalty of a larger absolute exposure energy.

A dramatic improvement in DOF and exposure latitude occurs as **A** is increased to 0.6. The bottom two Bossung curves show conditions of **A** equal to 0.6 and **n** equal to 3.0 and 6.0 respectively. Here, the normalized DOF range of 6 is near the total 24.0 micron range evaluated in the aerial simulation analysis. The flat DOF characteristics are evident at undersized conditions of a normalized CD of 0.8 for both photoresist designs. Of the two designs, the higher developer selectivity shows excellent exposure latitude in the normalized exposure range of 0.95 to 1.05, which is near the nominal spacewidth. In fact, the focus plots for these exposure energies are actually converging. This suggests that the size bias requirement for maximum exposure latitude is reduced from the previous designs. Since the simulated DOF actually exceeds the estimated theoretical DOF of 20.4 microns, it appears that the NLS requirement of 6.0 is too conservative for these last two photoresist designs.

3.0 Experimental Procedures

Two commercially available photoresist products, Hoechst Celanese AZ 4000 and Shipley STR 1000, were examined for their develop rate behavior, focus/exposure process windows and photoresist profiles. Both materials are specifically designed for thick photoresist applications. A high viscosity formulation of the AZ series, P 4620, was used for studying the 4, 5 and 10 micron thickness regimes, while P 4110 was used for 2 micron processes. A high viscosity formulation of the STR series, 1075 (44% solids) was used for 10 micron thickness regime, 1045 (38% solids) was used for the 4 and 5 micron regime and XP 90190 (21% solids) was used for the 2 micron processes. Optical properties of the AZ and STR series photoresists were provided by their respective manufacturers. The **A** value for the AZ series photoresists is 0.40 μm^{-1} at 436 nanometers, while the **A** value for the STR series photoresists is 0.31 μm^{-1} at 436 nanometers. These are small **A** values in comparison to high-contrast g and i-line photoresists used for thin-film applications.

An Ultratech Stepper Model 1700 was used for all experiments. The projection optics are based on the Wynne-Dyson-Hershel 1x lens design, with broadband illumination of the *g* and *h* mercury lines including the continuum from 390 to 450 nm. This system supports both a variable NA and partial coherence capability. A numerical aperture of 0.24 and partial coherence of 0.85 was used for all tests.

The photoresist coat and softbake processes were performed on a Solitec 5110C track system. Static dispensing techniques were used for all photoresist coating applications. Note that the spin time, acceleration and spin speed were intentionally varied in the experimental designs to achieve the desired film thickness.

Softbake processing was performed on either a Blue M convection oven or a MTI Flexifab hot plate bake system. For the AZ photoresist, a 105° C 45 minute convection bake was used while the Shipley STR used a 100° C 90 second hot plate bake.

Photoresist development processing was performed using a batch immersion method with constant agitation at room temperature. The AZ 4000 series photoresist was developed using AZ 400K developer mixed in a 5:1 ratio with dionized (DI) water, which provided a 0.23 N solution. The Shipley STR 1000 series photoresist was developed using premixed Shipley 452 developer.

4.0 Experimental Results

4.1 Develop Rate Results

The develop rate characteristics for the two families of photoresists were measured at 2, 5 and 10 micron thicknesses. Develop rate data was determined using standard open frame dose clear methods (contrast curves). A range of 50 to 650 mJ/cm^2 exposures in 15 mJ increments were used for each case. This range of exposures was repeated for a matrix of develop times. For the 2

micron film thicknesses, develop times of 1 to 4 minutes were performed in half-minute steps. Develop times of 2, 2.5, 3, 3.5, 4, 4.5, 5, 6 and 8 minutes were performed for the 5 micron photoresist thicknesses, while develop times of 3, 4, 5, 6, 7, 8, 9, 10 and 12 minutes were used for the 10 micron photoresists. Resulting film thicknesses were measured using an Alpha step stylus profilometer.

Photoresist develop rates were then calculated for each exposure energy from film thickness versus develop time rate curves. This provided an effective average develop rate for a given film thickness and exposure dose. A corresponding average Photo Active Compound (PAC) concentration was then determined for the various exposure energies and film thicknesses. Photoresist development rate versus relative PAC is shown in Figures 7 and 8 respectively for the Shipley STR 1000 family and AZ 4000 family photoresists. Graphs (a), (b) and (c) show the initial film thicknesses of 2, 5 and 10 microns respectively.

The develop rate model proposed by Trefonas and Mack was fit to the experimental data [9]:

$$\text{Rate} = R_{max}\,(1 - e^{-EC})^{\,n} + R_{min} \qquad (2)$$

where $\mathbf{R}_{max}$ is the maximum develop rate of fully exposed photoresist, $\mathbf{R}_{min}$ is the unexposed develop rate, **n** is the developer selectivity, **E** is the exposure dose and **C** is the effective photoresist rate constant. The term e^{-EC} is equivalent to the relative PAC concentration [9], hence equation (2) can be fit to the experimental results to determine the develop rate parameters.

The develop rate parameters determined from the regression analysis are summarized in Table 3. For the AZ 4000 family of photoresists, the experimentally determined $\mathbf{R}_{max}$ values were found to be on the order of 30 to 60 nm/sec. The value for the STR 1000 family was slightly higher-around 60 to 75 nm/sec. Note that the exposure doses used in the experiment did not fully encompass high PAC conversion for the thicker photoresist case of 10 microns. One clear trend of the develop rate behavior with increasing film thickness is an apparent steepening of the rate versus relative PAC concentration.

One of the significant differences between the two photoresist products is the **n** value. The STR 1000 family shows **n** values of approximately 4.5 to 5.0 while the AZ 4000 family has **n** values around 1.2 to 2.5. Based on the simulation results, the higher **n** values of the STR 1000 family should provide enhanced exposure latitude and focus latitude compared to the AZ 4000 family.

4.2 Focus/Exposure Results

Cross sectional SEM analysis was used to evaluate the quality of 4 micron line and space patterns in 2, 4, 5 and 10 microns of photoresist as a function of focus. The 2, 4 and 10 micron results for the STR 1000 family and the AZ 4000 family are shown in Figures 9 and 10 respectively. The displayed focus range for the STR family is approximately 16 microns, while the range for the AZ family is approximately 12.5 microns. It is apparent that the STR 1000 family shows better wall angle and CD control over a larger range of focus than the AZ 4000 family. This can be directly correlated to the differences in **n** values for STR 1000 photoresists and AZ 4000 photoresists as

discussed in the previous section. It is interesting to note for thick films that both photoresist families show a "milk bottle" profile for large negative defocus. This confirms the model simulations indicating that a large negative defocus should have the poorest exposure latitude.

Complete SEM analysis was performed to collect CD data as a function of both focus and exposure for both photoresist families. Next, all of the data was normalized to allow easier performance of relative comparisons among the various photoresist thicknesses.

Bossung plots for a 4 micron spacewidth in 2, 5 and 10 microns of STR 1000 family are shown in Figure 11. The 2 micron photoresist shows the classic Bossung pattern with concave and convex curves as a function of exposure. In contrast, the thicker photoresists show a flat CD response through focus at high exposures. Only the low exposures show a convex profile, and the center of the curve is offset from the zero focus. The focus offset corresponds to the isofocal point for the thick photoresist films.

Bossung plots for a 4 micron spacewidth in 2, 5 and 10 microns of AZ 4000 family are shown in Figure 12. The 2 micron photoresist curves show an unusual nonsymmetric response between positive and negative focus offsets. Bossung plots for the thicker AZ 4000 series photoresists show a large variability in CD as a function of focus suggesting a poor process latitude. The large amount of scatter in the results masks any convex or concave curvature trends.

4.3 Thickness Comparisons

Process latitude was selected as a metric to compare thickness effects for the two photoresist families. The Bossung plots from the previous section were used to determine the maximum focus and exposure process ranges within an industry-standard 10% CD criteria. Figure 13 shows the normalized focus range (DF/S) as a function of thickness for STR 1000 and AZ 4000 photoresists. Both figures show a reduction in focus range as the photoresist thickness is increased. However, the reduction in focus range is much more rapid with the AZ 4000 series. It appears to be essentially flat in the 4 to 10 microns thickness regime.

Figure 14 shows the normalized exposure range ($\Delta E/E_n$) as a function of thickness for STR 1000 and AZ 4000 photoresists. The STR 1000 series shows a characteristic reduction in exposure range with increasing photoresist thickness. In contrast, the AZ 4000 series is relatively flat with some large outliers due to the noise in the Bossung plots. Overall, the exposure latitude for the AZ 4000 series is less than for the STR 1000 series.

5.0 Discussion and Conclusions

It is useful to compare the simulation and experimental results from this study for understanding the important properties in thick photoresist applications. First, as predicted in section 1.0, both photoresists show a loss in DOF as thickness is increased. At a film thickness of 2.0 microns, there is a maximum DOF range of 16 microns, which compares to a predicted value of

approximately 19 microns from Figure 3. At a film thickness of 10 microns, the DOF is 8.5 microns. Increasing film thickness from 2 to 10 microns degrades normalized DOF for both photoresists as predicted by simulations. However, the normalized exposure latitudes are less sensitive to an increase in film thickness.

Using simulation modeling in conjunction with factorial design methodology has shown the importance of the photoresist absorption parameter **A** (μm^{-1}) and the developer selectivity **n** in determining lithographic performance for a 10 micron film. High values of **n** equal to 6.0 provide increased process latitude, while low values of **A** equal to 0.2 reduce the required exposure energy. As **A** is increased to 0.60 exposure the focus latitude increases further. Therefore, depending on the specific process requirements, it is recommended to design a thick resist with either a low or high **A** value along with a high developer selectivity.

Experimental develop rates were obtained for two commercial photoresist products, Hoechst Celanese AZ 4000 and Shipley STR 1000. Develop rate results show a large difference in the **n** value between these two materials. The cross sectional SEM analysis and Bossung plots for all three films thicknesses indicate that the STR 1000 family has a larger focus and exposure margin than AZ 4000. This supports the simulation predictions of the importance of developer selectivity **n** in lithographic performance.

6.0 References

1. Kryder, M., “Data-Storage Technologies for Advanced Computing”, *Scientific American*, Vol. 257 (4), October 1987, pp. 117-125.

2. Gau, J., “Photolithography for Integrated Thin-Film Read/Write Heads”, *Optical/ Laser Microlithography II*, Proc. SPIE Vol. 1088 (1989), pp. 504-514.

3. Flores, G., Flack, W., Dwyer, L., “Lithographic Performance of a New Generation i-line Optical System”, *Optical/Laser Lithography VI*, Proc. SPIE Vol. 1927 (1993).

4. Mack, C. et. al., “Modeling and Characterization of a 0.5 mm Deep Ultraviolet Process”, *J. Vac. Sci. Technol.*, B 9 (6) (1991), pp. 3143-3149.

5. Mack, C., “An Algorithm for Optimizing Stepper Performance Through Image manipulation”, *Optical/Laser Microlithography III*, Proc. SPIE Vol. 1264 (1990), pp. 71-82.

6. Mack, C., “New Kinetic Model for Resist Dissolution”, *J. Electrochem. Soc.*, 139 (4) (1992), pp. L35 - L37.

7. Flores, G., Flack, W., Tai, E., Mack, C., “Lithographic Performance in Thick Photoresist Applications”, *OCG Microlithography Seminar, Interface '93 Proceedings*, (1993) pp. 41-59.

8. Box, G., Hunter, W., Hunter, J., Statistics for Experimenters, Wiley Interscience, John Wiley and Sons, New York (1978).

9. Trefonas, P., Mack, C., "Exposure Dose Optimization for a Positive Resist Containing Polyfunctional Photoactive Compound", *Advances in Resist Technology and Processing VIII,* Proc. SPIE Vol. 1466 (1991) pp. 270 - 282.

Factor	Low	High
Absorption Parameter **A** (μm^{-1})	0.2	0.6
Develop Selectivity **n**	3.0	6.0

TABLE 1. Factorial design conditions used for process simulation studies.

Parameter	Setting
Optical System numerical aperture	0.24
Partial coherence	0.85
Illumination bandwidth (nm)	400 - 440
Photoresist parameter **B** (μm^{-1})	0.05
Photoresist parameter **C** (cm^2/mJ)	0.016
Index of refraction	1.65
Substrate type	silicon
PEB Diffusion length	0
Maximum Develop Rate: R_{max} (nm/sec)	200
Minimum Develop Rate: R_{min} (nm/sec)	0.1
Threshold PAC concentration m_{th}	-10
Develop time (sec)	300

TABLE 2. Simulation parameter values for process simulation studies.

Resist	Thickness (μm)	n	R_{max} (nm/sec)	R_{min} (nm/sec)
AZ 4000	2	2.1	30	0.5
AZ 4000	5	2.5	60	2
AZ 4000	10	1.2	30	1
STR 1000	2	4.4	63	0.5
STR 1000	5	5.0	55	3
STR 1000	10	4.5	75	2

TABLE 3. Experimental develop rate parameters.

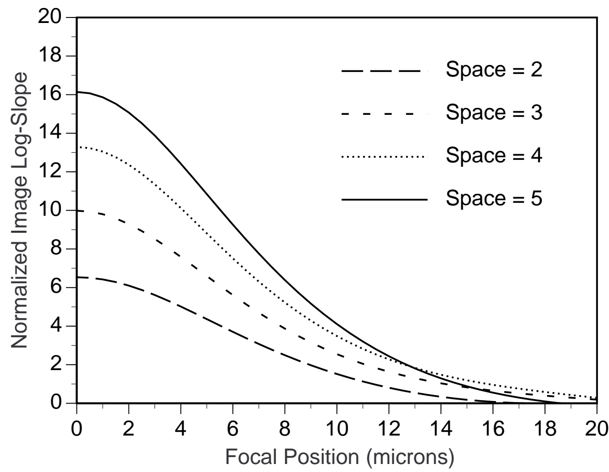

Figure 1: Normalized image log-slope versus focal position for constant pitch of 7 micron at 2,3,4 and 5 micron. spacewidths. Numerical aperture of 0.24.

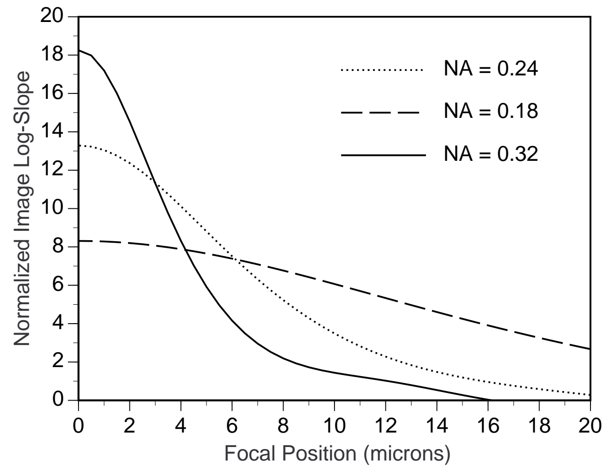

Figure 2: Normalized image log-slope versus focal position for a 4 micron spacewidth and 7 micron pitch at numerical apertures of 0.18, 0.24 and 0.32.

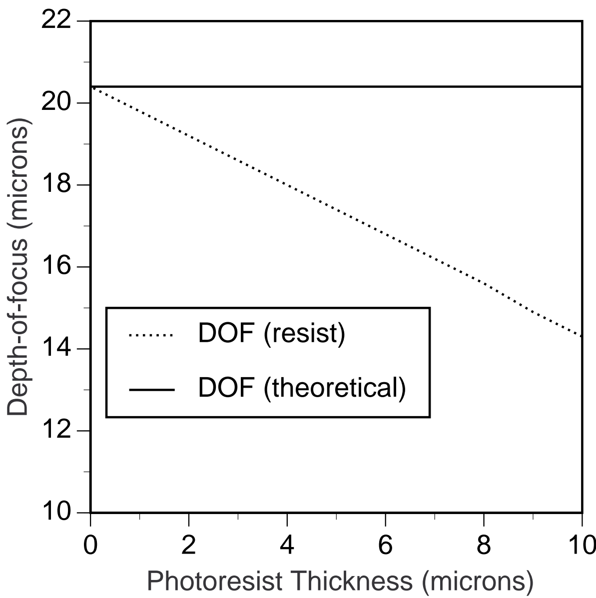

Figure 3: Depth-of-focus versus photoresist thickness for a 2 micron spacewidth and 7 micron pitch at a numerical aperture of 0.24.

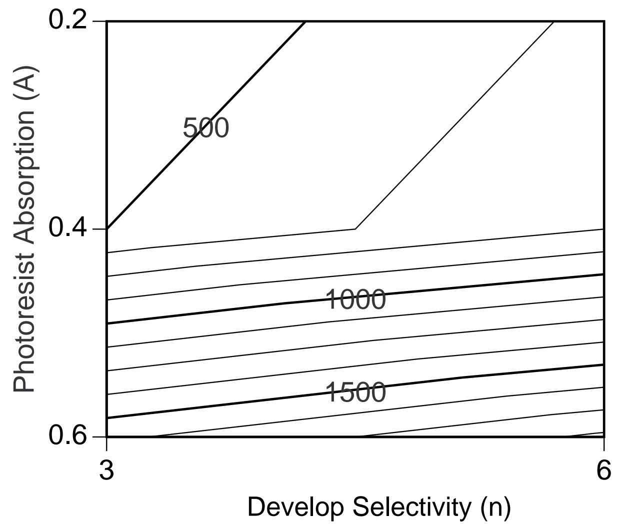

Figure 4: Contour plot of dose to size as a function of photoresist absorbance A and develop selectivity ***n****.*

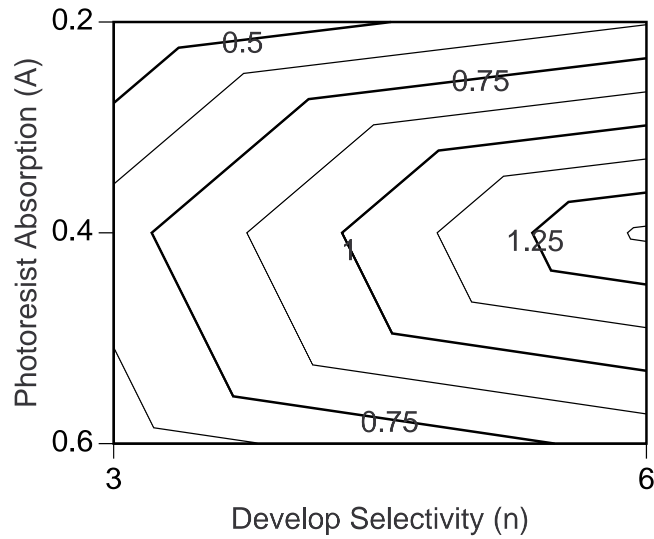

*Figure 5: Contour plot of normalized exposure latitude as a function of photoresist absorbance **A** and develop selectivity **n**.*

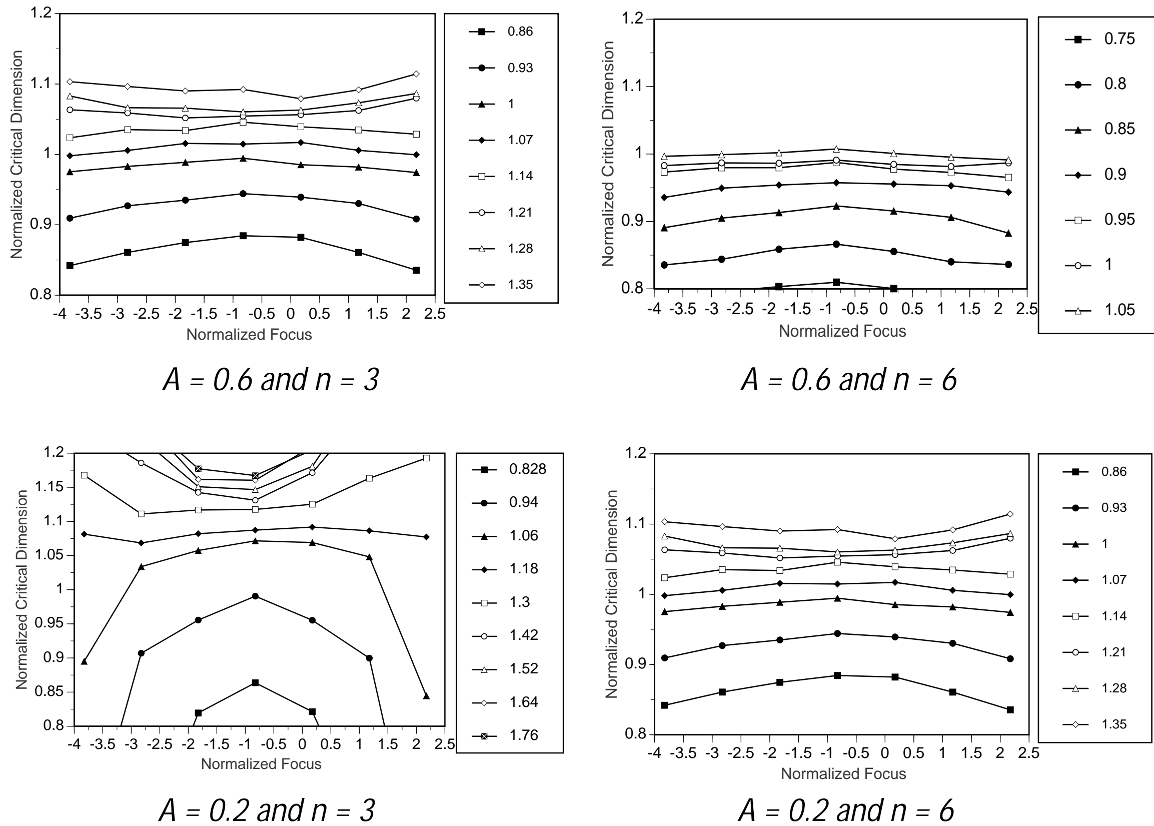

Figure 6: Simulated Bossung curves at four extreme conditions for the factorial design.

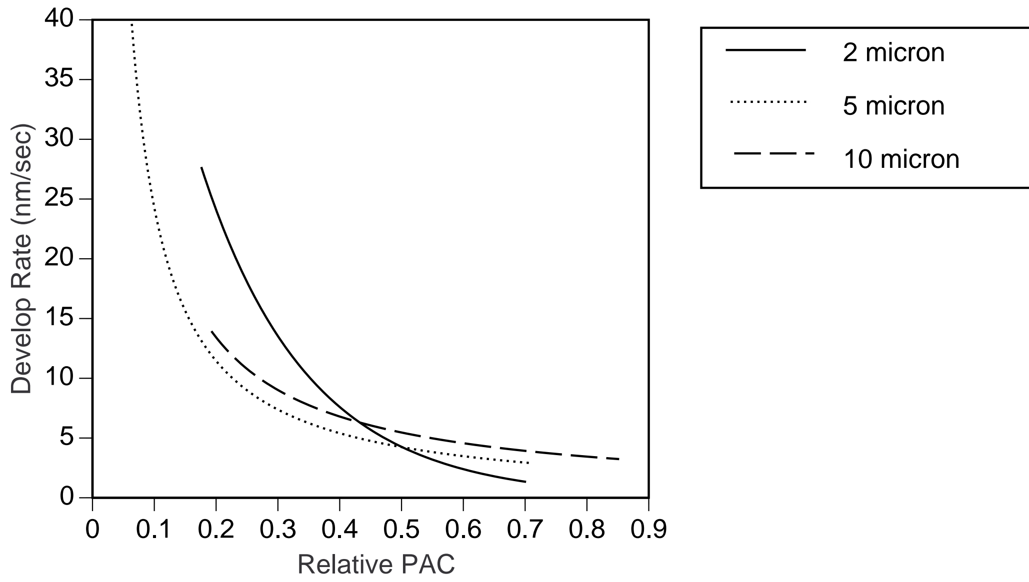

Figure 7: Develop rate versus PAC for Shipley series photoresists.

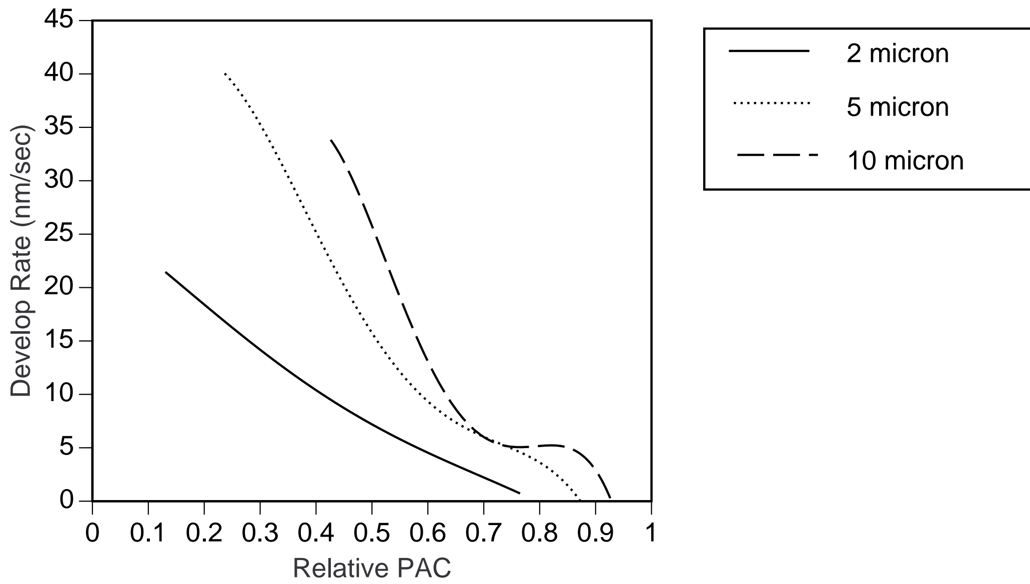

Figure 8: Develop rate versus PAC for AZ series photoresists.

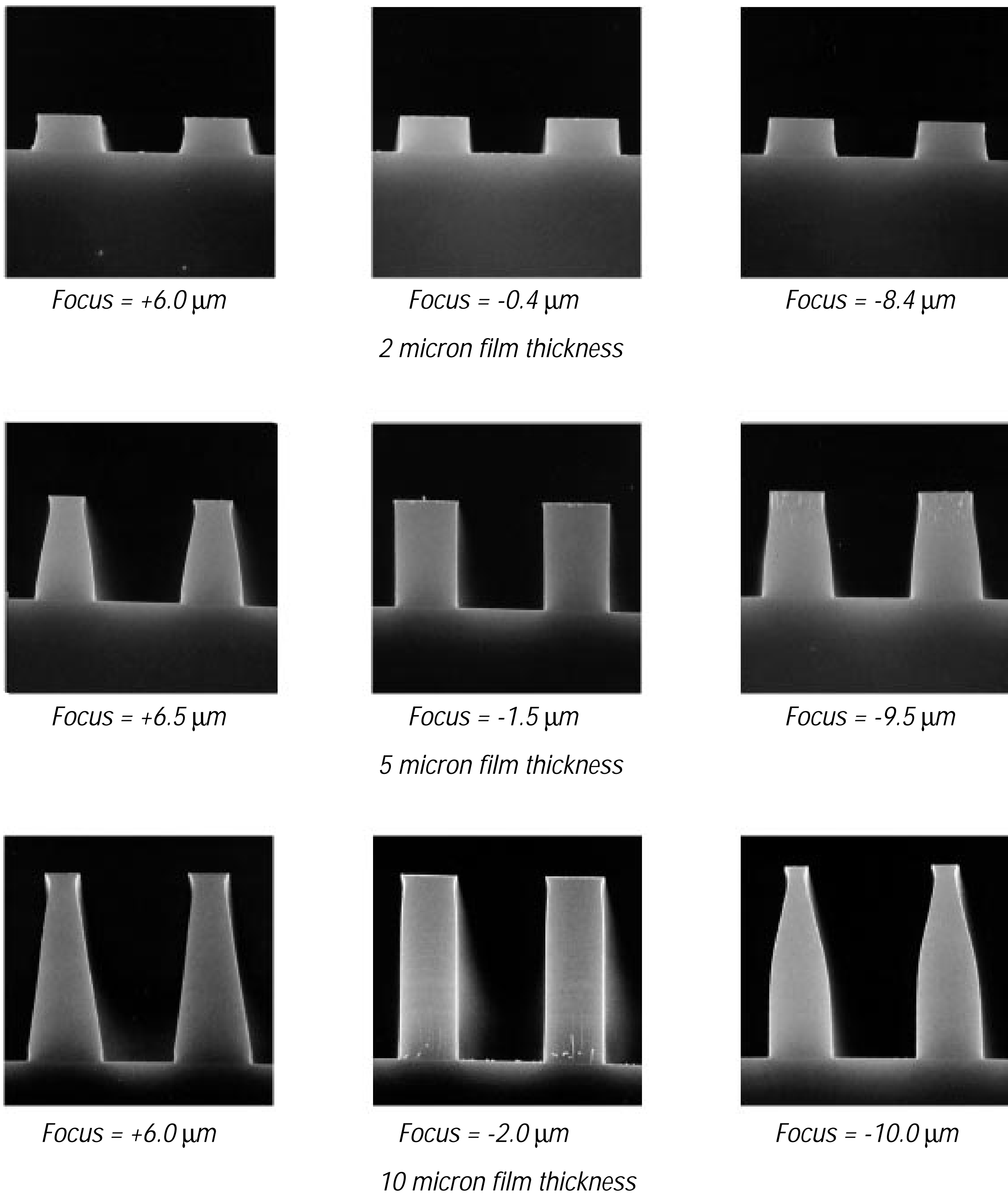

Figure 9: Depth of focus comparison of 4 micron lines and spaces in 2, 5 and 10 microns of Shipley STR series photoresists.

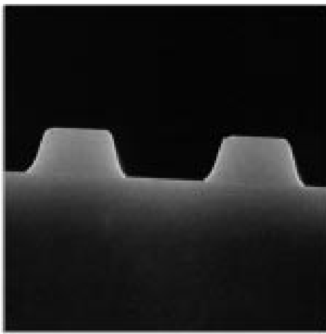

Focus = +5.5 µm

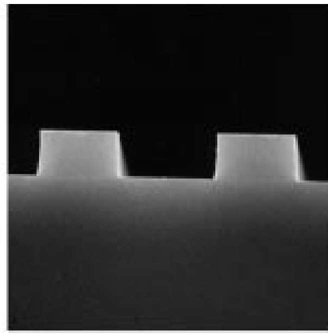

Focus = -0.75 µm

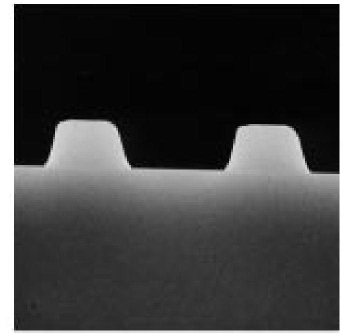

Focus = -7.0 µm

2 micron film thickness

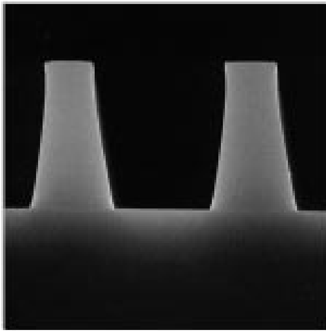

Focus = +4.75 µm

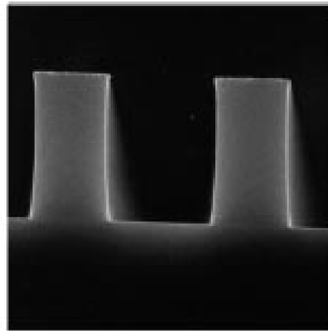

Focus = -1.5 µm

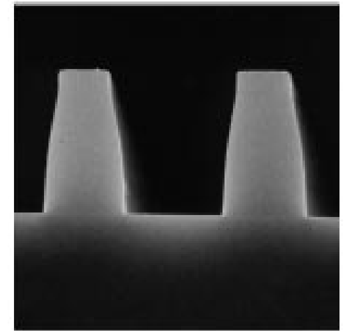

Focus = -7.75 µm

5 micron film thickness

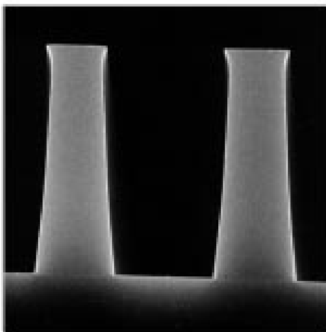

Focus = +3.0 µm

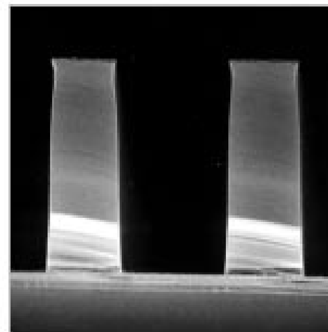

Focus = -3.25 µm

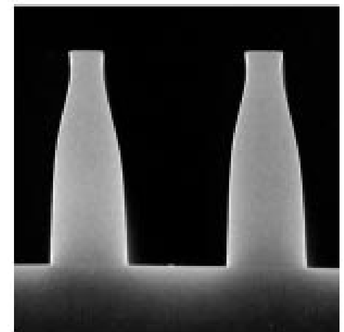

Focus = -8.25 µm

10 micron film thickness

Figure 10: Depth of focus comparison of 4 micron lines and spaces in 2, 5 and 10 microns of AZ series 4000 photoresists.

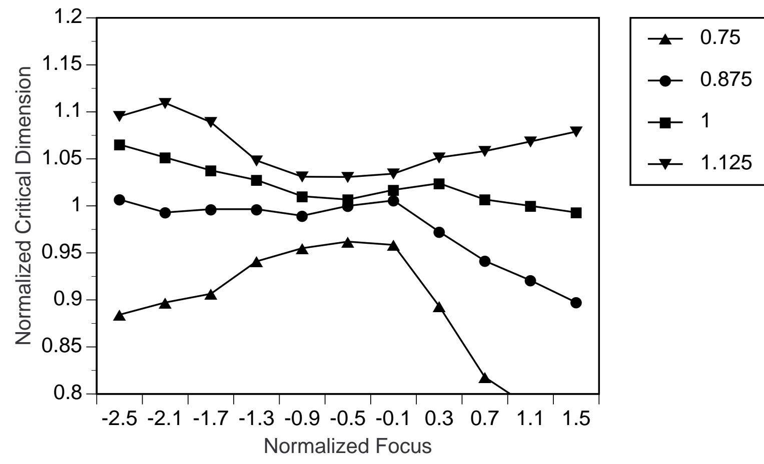

2 micron film

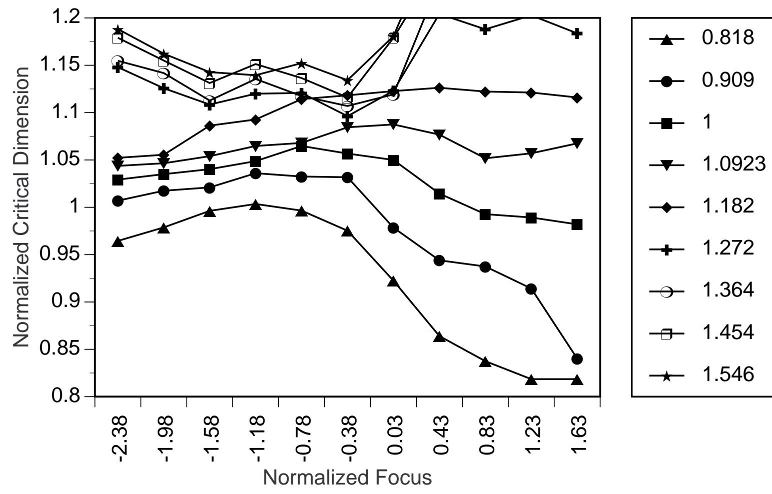

5 micron film

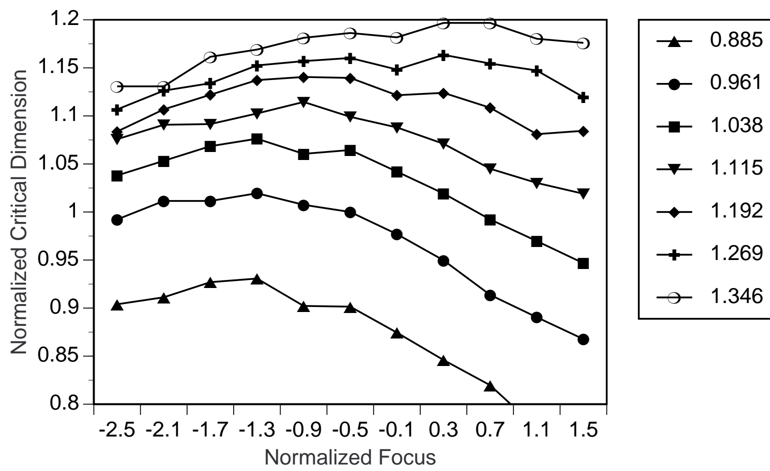

10 micron film

Figure 11: Experimental normalized Bossung plot of Shipley series STR at 2, 5 and 10 micron film thicknesses.

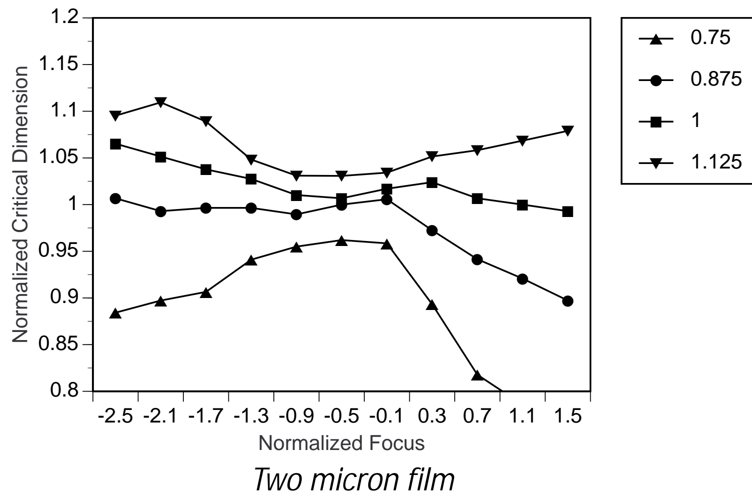

Two micron film

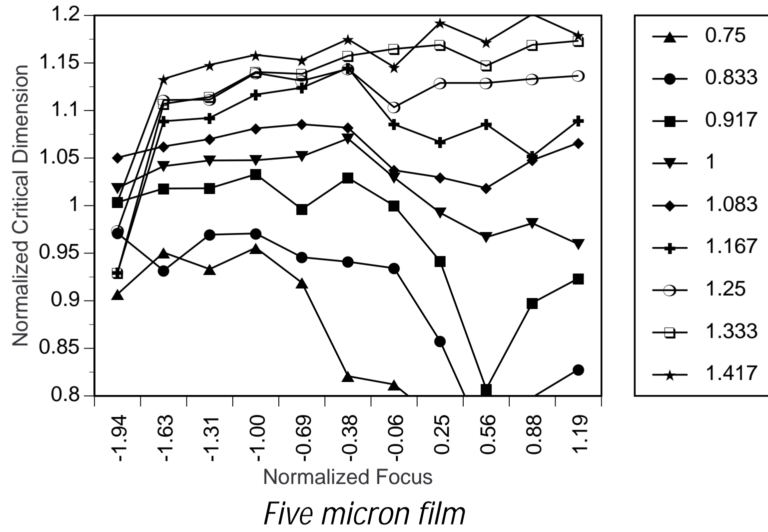

Five micron film

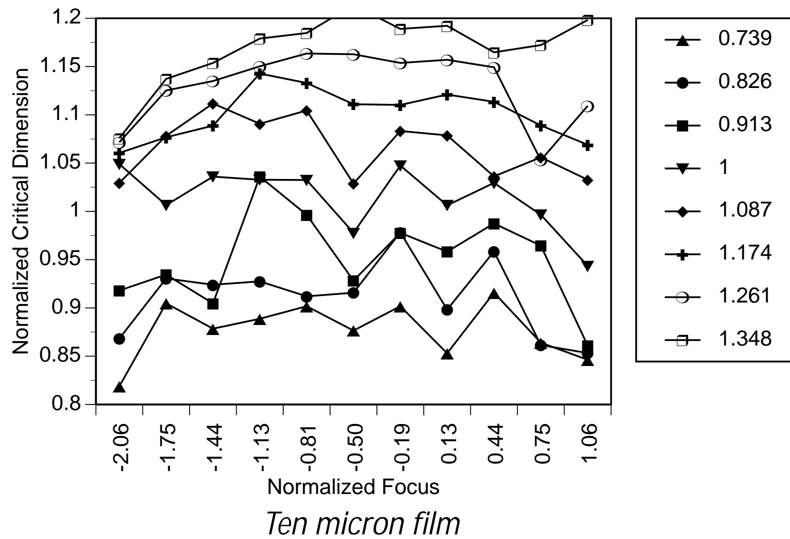

Ten micron film

Figure 12: Experimental normalized Bossung plot of AZ series 4000 at 2, 5 and 10 micron film thicknesses.

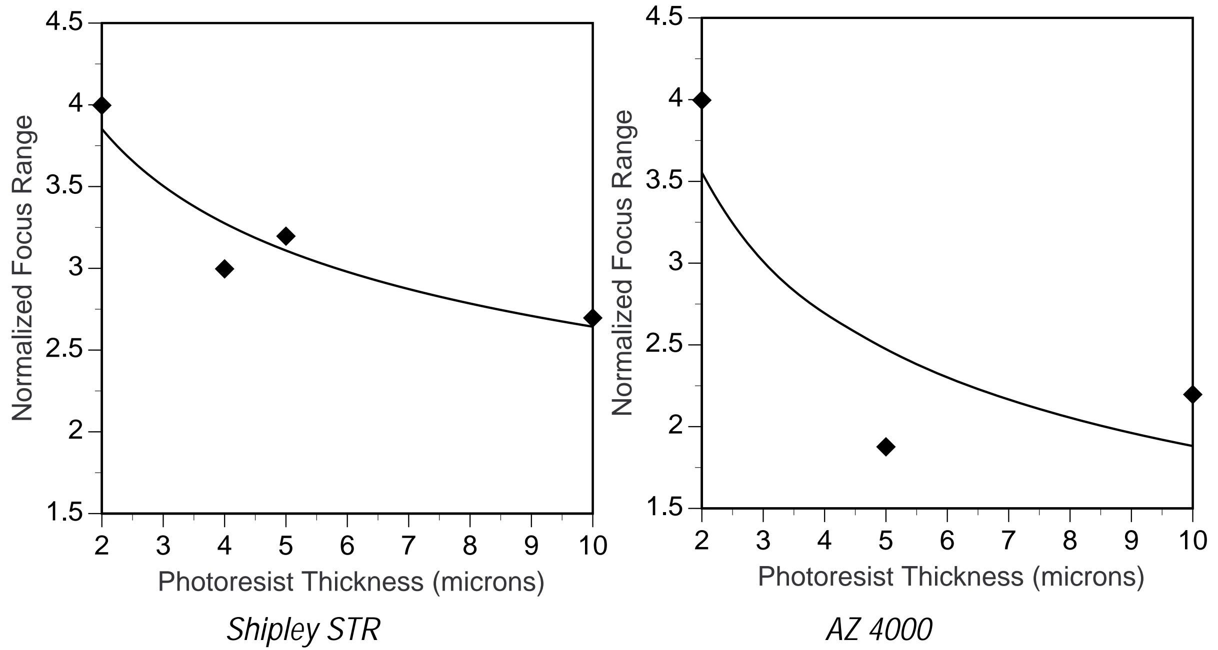

Figure 13: Normalized depth of focus versus photoresist thickness for the Shipley STR and the AZ 4000 photoresists.

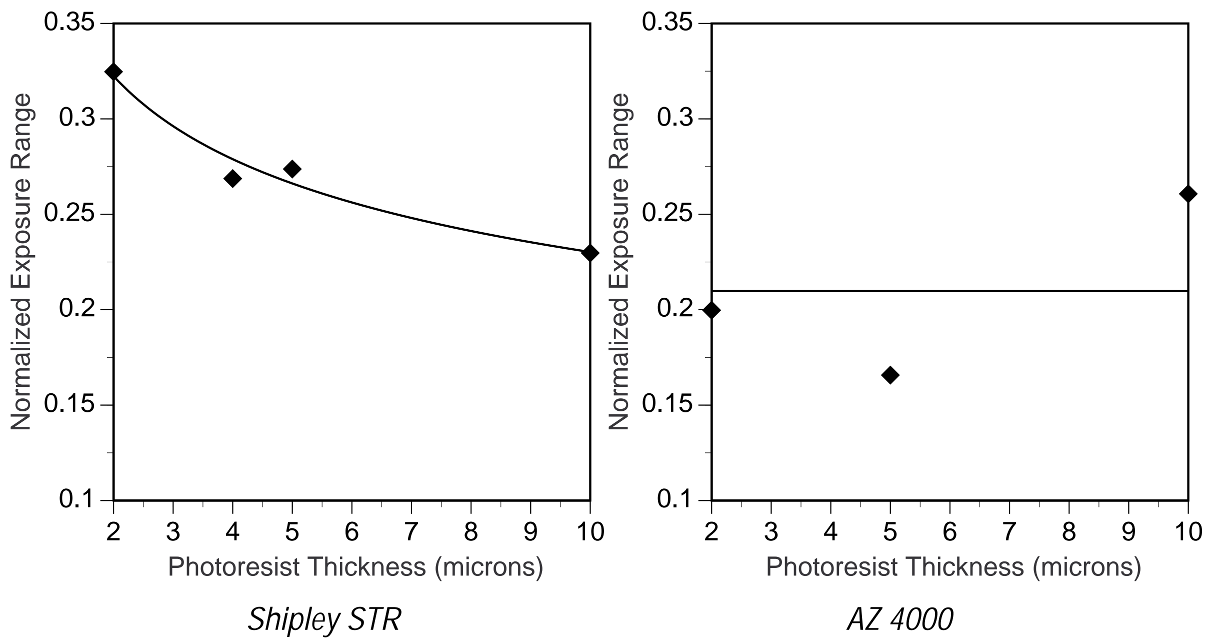

Figure 14: Normalized exposure latitude versus photoresist thickness for the Shipley STR and the AZ 4000 photoresists.